CHEMICAL ENGINEERING TRANSACTIONS
VOL. 64, 2018
A publication of AIDIC
The Italian Association of Chemical Engineering
Online at www.aidic.it/cet
Guest Editors: Enrico Bardone, Antonio Marzocchella, Tajalli Keshavarz

ISBN978-88-95608- 56-3; **ISSN** 2283-9216

Novel Kojic Acid-Based Functionalized Silica Nanoparticles for Tyrosinase and Ache Inhibition and Antimicrobial Applications

Gesiane da S. Lima[a], Gracielle F. Andrade[b], Mirra A. N. da Silva[a], Edésia M. B. de Sousa[b], Jacqueline A. Takahashi*[a]

[a]Departamento de Química, Universidade Federal de Minas Gerais , Av. Presidente Antonio Carlos, 6.627, 31270-901, Belo Horizonte, MG, Brazil.
[b]Serviço de Nanotecnologia, Centro de Desenvolvimento da Tecnologia Nuclear, Av.Presidente Antonio Carlos, 6.627, 31270-901, Belo Horizonte, MG, Brazil
jat@qui.ufmg.br

Cultivation of the fungal species *Aspergillus parasiticus* led to the isolation of Kojic acid (KA), an important secondary metabolite, but unstable under some conditions. In order to improve the pharmacokinetic potential of KA for biotechnological applications in pharmaceutical and cosmetic formulations, KA was immobilized in mesoporous nanomaterials based on silica (MSN). This kind of inorganic support has been intensively studied as candidates for controlling-release drugs, due to its high surface area, high ordering of mesopores and pore size in nanometer scale. In this way, mesoporous silica nanoparticles have been synthesized and were chemically modified by post-synthesis with 3-aminopropyltriethoxysilane (MSNAPTES) and the influence of functionalization of the matrix on the loading rate of KA was studied. Nanoparticles were physicochemical characterized by SAXS, SEM, CHN, TGA, N_2 adsorption, photon correlation spectroscopy and zeta potential analysis. Bactericidal efficacy of these nanoparticles was tested against different microorganisms, and these new kojic acid nanoparticles showed high bactericidal efficiency. In relation to acetylcholinesterase (AChE) inhibition test, used to screen drugs active to treat Alzheimer's disease patients, MSNAPTES KA nanoparticles showed to be as efficient as the free-acid. KA loading showed also tyrosine inhibitory property preserved. The results points that, although free-kojic acid amount in MSNAPTES KA is thirty times lower, biological activity of this nanoparticle is as high as the activity of free-kojic acid, being, therefore, a highly and multi-active nano-system for kojic acid delivery with improved pharmacokinetic skills and a wide scope of industrial applications.

1. Introduction

Kojic acid (KA) is a secondary metabolite produced by fermentation from various microorganisms, including fungi of *Aspergillus genus*. This important biotechnological product was isolated for the first time from *Aspergillus oryzae*, in Japan (Burnett et al., 2010) where KA is widely used in the traditional foodstuffs production, like *saké*, *shoyu* and mirin and can also be applied as a food preservative and precursor for flavor enhancers (Bentley, 2006). KA has several biological properties such as antimicrobial (Nohynek et al., 2004), anti-inflammatory and antioxidant (Bentley, 2006). Therefore, KA has application in several industrial areas.
In cosmetics industry, use of KA in formulations of whitening creams, skin protective lotions and other related products has grown over the years. In this area, this acid plays important functions, among them ultra violet filtration, tyrosinase inhibitory activity, radical scavenging activity and radio-protective function.
In addition, the Food and Drug Administration (FDA, USA) approved the use of KA associated with other compounds for dermatological treatment purposes (Mohamad et al., 2010). FDA points the use of KA in cosmetic and dermatological formulations in a numerous of countries like the United States, Canada, Chile, India, South Korea, and other Asian countries, alone or in combination with other products. In Japan KA-containing products are regulated and classified as *quasi-drugs* (FDA, 2016). According to the FDA there are

more than twenty products on the market that take between 1 to 5% of KA in their formulations that are applied as skin lightener, like AHA Lightening Gel® a cream formulated with 2% of KA produced by Dermatologic Cosmetic Laboratories (DCL) in Singapore.
Due to the importance of KA as tyrosinase and antimicrobial inhibitor and to the potential for other applications, this compound was chosen as a model in our laboratory. In order to improve the pharmacokinetic potential of KA in pharmaceutical and cosmetic formulations, KA was immobilized in mesoporous silica based nanomaterials (MSN). This inorganic support has been intensively studied as a candidate for controlling drugs release, due to its high surface area, high ordering of mesopores and pore size in nanometer scale (Vallet-Regi et al., 2001). In this way, MSN have been synthesized and post-synthesis modified with 3-aminopropyltriethoxysilane (MSNAPTES). Influence of chemical modification of the matrix on the loading rate of KA drug was studied. Then, the profile of biological activities of KA-nanoparticles was evaluated.

2. Methods

2.1 Microorganism, cultivation and extract obtained

Aspergillus parasiticus strain was isolated from soil and maintained on potato dextrose agar (PDA) at 4 ^{o}C. Fungal strain was inoculated in (g/L): glucose, 20; sucrose, 150; yeast extract, 12; $MgSO_4.7H_2O$, 0.5 medium in 500 mL Erlenmeyer flasks, at room temperature, for 14 days on a rotary shaker at 1 G (triplicate). After incubation, culture broth was separated from mycelium by vacuum filtration and liquid phase was extracted with ethyl acetate (3x). The resulting organic fractions were combined, concentrated under vacuum and the resulting extract was stored under refrigeration.

2.2 Kojic acid obtaining and characterization

The extract presented crystals in the form of needles. Small amount of methanol was added and solid material was separated from the remaining brown soluble constituents of the extract after cooling the material in a refrigerator at 5 ^{o}C for 24 h. The crystalline material was filtered off, excess of solvent was removed, the crystals were dried. The reminiscent solvent was submitted to successive crystallization processes with acetone-methanol mixture. Pure KA obtained was characterized by Nuclear Magnetic Resonance (^{1}H and ^{13}C NMR) spectroscopy.

2.3 Synthesis of mesoporous silica nanoparticles and functionalization of MSN with 3-aminopropyltriethoxysilane (APTES)

Silica nanoparticles were synthesized using CTAB that were dissolved in 450 mL of NaOH solution. Then, a mixture of 5 mL of tetraethylorthosilicate was added to the solution under constant stirring at 80 °C for 2 h. The solids obtained were collected by centrifugation and dried under open air flow at 37 °C. The surfactant was removed by calcination, which was carried out by increasing the temperature to 550 °C for 5 hours (Fan, 2011). Functionalization process has been performed through reaction between the silica mesoporous material and APTES, under reflux in toluene, according to the methodology previously described (Izquierdo-Barba et al., 2009).

2.4 Physicochemical and morphological characterization of MSN, MSNAPTES and MSNAPTES KA

Samples were physicochemically characterized by small angle X-ray scattering (SAXS), scanning Electron microscopy (SEM), elemental analysis (CHN), thermogravimetric (TGA), N_2 adsorption/desorption, photon correlation spectroscopy and zeta potential analysis. The small-angle X-ray diffraction patterns were recorded on Rigaku, Ultima IV, and powder diffractometer using CuKα radiation. Functionalization process was analysed by TGA and elemental analysis. TGA measurements were taken by a Shimadzu TGA 50WS (25 to 700°C) with nitrogen (N_2) atmosphere flow of 50 mL min^{-1}. Elemental analysis was performed in a Perkin–Elmer CHNSO model 2400. Nitrogen adsorption isotherms of samples were obtained at 77 K using a QuantachromeSiQwin™- Automated Gas Sorption Data adsorption analyser. All data analyses were performed using NovaWin, 1994–2011 Quantachrome Instruments software (Boynton Beach, FL, USA). The analytical procedure to perform photon correlation spectroscopy and zeta potential analysis was conducted in a ZetasizerNanoseriesZs (Malvern Instruments, Malvern, UK) apparatus after its adequate dilution in ultra-pure MilliQwater (pH 7.0). The SEM images were captured on a Quanta 200-FEG-FEI-2006 microscope.

2.5 Kojic acid loading

Adsorption of kojic acid within MSNAPTES was performed by soaking 100 mg of the powder sample in a kojic acid solution (1000 μg mL^{-1}) kept under magnetic stirring for 120h. The obtained mixture was filtered. The uptake kojic acid by the mesoporous materials was estimated by TG and CHN, and the loaded amount of kojic acid in the nanoparticle was 3%.

2.6 Acetylcholinesterase (AChE) inhibitory assay

This assay was carried out on 96 wells microplates based on Ellmann's method with modifications (dos Santos et al., 2017). Firstly, 125 µL of DTNB solution, 50 µL of buffer Tris/HCl solution, 25 µL of ATCI and 25 µL of sample in dimethylsulfoxide (1 mg mL^{-1}) were added in each well. Absorbance of the mixture was measured at 405 nm every 60 s, 8 times. Then, 25 µL of AChE solution were added. Absorbance was measured again every 60 s, 10 times. Galantamine was used as positive control and DMSO as negative control. All assays were carried out on quintuplicate and the percent inhibition of AChE was calculated as follows: Inhibition (%) = 100-[(RSsample / RBcontrol)*100], where RSsample = rate of sample extracts reaction and RBcontrol = rate of blank.

2.7 Tyrosinase assay

Tyrosinase inhibition was performed by spectrophotometric method with modification (Ashraf et al., 2015). PBS buffer solution (80 µL) (20 mM, pH 6.8) was added to 20 µL of sample (in DMSO, 500 µg mL^{-1}) and 50 µL of L-DOPA (3, 4-dihidroxifenilalanin; 0.85 mM). Mixture was incubated for 15 min at 25 ^{o}C and absorbance was measured at 450 nm. Then, 50 µL of mushroom tyrosinase solution (57.7 U/mL) was added in each well. Mixture was incubated and absorbance was measured again. KA was used as positive control and DMSO as negative control. Percentage of inhibition was calculated by this formula: Inhibition (%) = [(A-B) –(C-D) / (A-B)]*100], were A = absorbance of negative control with enzyme, B = absorbance of negative control without enzyme; C = absorbance of the sample with enzyme, D = absorbance of the sample without enzyme.

2.8 Antimicrobial assay

Microorganisms used in this study were *Salmonella enterica* (ATCC 14028), *Bacillus cereus* (ATCC 11778), *Escherichia coli* (ATCC 25922), *Staphylococcus aureus* (ATCC 29213) and *Candida albicans* (ATCC 18804). Methodology described in CSLI norm for bacteria and yeasts with minor modifications, was applied and all compounds were tested at 1 mg mL^{-1} (in DMSO). All experiments were carried out in triplicate in 96 wells plates. Absorbance was measured at 485 nm and results are expressed as percent of inhibition in relation to the blank (plate without compounds tested). Chloramphenicol and itraconazole were used as positive control for the bacteria and yeast assay, respectively. DMSO was used as negative control.

3. Results and discussion

3.1 Small-angle X-ray scattering (SAXS) and N_2 adsorption/desorption

Figure 1(a) shows the SAXS patterns confirming highly ordered materials. MSN sample revealed one intense peaks related to the (100) at 2θ=2.5 and two other less intense peaks related to the (110) and (200) diffraction planes. It is noteworthy that functionalized samples also exhibit a well-resolved peak indexed as (100), typical of ordered hexagonal mesoporous structures. However, main SAXS reflection intensity maintain after hydrocarbon chain incorporation in MSNAPTES sample. Figure 1(b) shows N_2 adsorption/desorption isotherms. All samples exhibit a type IV isotherm characteristic of mesoporous materials. As expected, the introduction of the organic moieties, APTES, leads to a decrease in surface area. This decrease evidences the fact that organic material is located within the pores of the matrices. It should be noted that BET surface area of MSN decreased from 1216 to 148 $m^2.g^{-1}$ (MSNAPTES), after surface modification with APTES. Pore diameter value calculated from DFT method for MSN and MSNAPTES was 3.0 nm. MSN and MSNAPTES pore volume values that were calculated from DFT method are 0.316cm^3 g^{-1} and 0.127cm^3 g^{-1}.

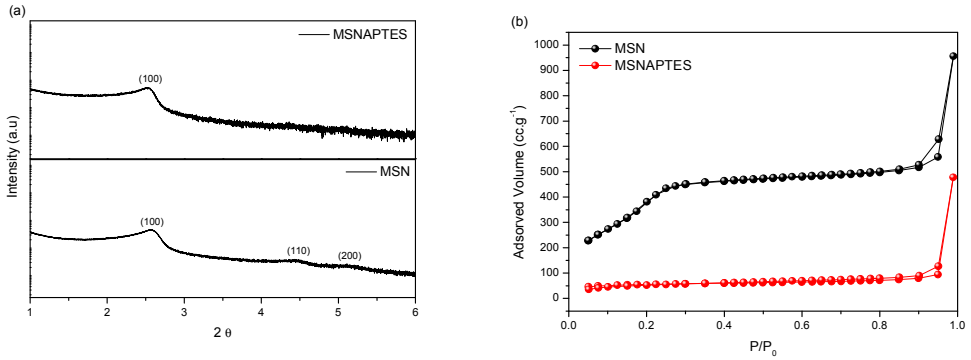

Figure 1: (a) SAXS patterns of MSN and MSNAPTES samples; (b) Nitrogen adsorption-desorption isotherms.

3.2 Thermogravimetry analysis (TGA) and elemental analysis (CHN)

TGA curves of all the systems are shown (Fig. 2) and results are summarized in Table 1. The pure sample showed initial weight loss of 3.8 from 25 to 150 °C, which is apparently due to the thermodesorption of physically adsorbed water. Above 150 and up to 700 °C, weight loss was around 3.1% and corresponds to silanol groups condensation (Kim et al., 2009). The MSN material has adequate thermal stability for the proposed application, justifying to conduction of biological assays. The amount of functionalized agent anchored in the MSNAPTES sample as well as the amount of kojic acid incorporated inside of this matrix was estimated by TGA technique (Table 1). In the cases of functionalized samples, weight loss occurred in two distinct regions for all samples. First region of mass loss occurs in temperature range between 25 and 150 °C, which can be attributed to thermodesorption of physically adsorbed water. The second region showed weight loss between 150 and 700°C, which can be attributed to decomposition temperature for incorporated alcoxysilane groups and kojic acid loaded. Another evidence on the surface modification with APTES and incorporation of kojic acid in the MSNAPTES matrix was obtained through elemental analysis. This technique indicates an increase in the percentages variation of the carbon element (%C) in MSN where APTES functionalization and kojic acid loading occurred. Table 1 shows the values for contents of this element contained in the matrices after APTES anchoring and kojic acid loading. The results indicate that APTES group and kojic acid were incorporated in the structure of MSN.

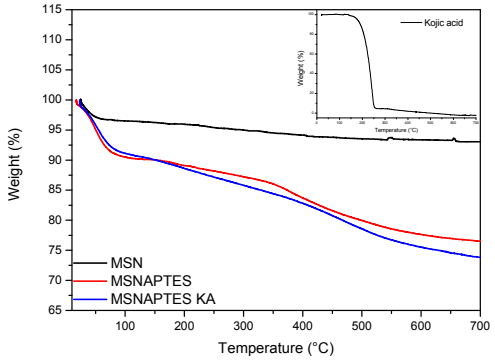

Figure 2: TG curves of MSN, MSNAPTES and MSNAPTES KA samples.

3.3 Photon correlation spectroscopy and Zeta potential analysis

Zeta potential measurements are used to characterize the surface charges of particles. Table 1 shows the values of zeta potential measurements for MSN, MSNAPTES and MSNAPTES KA samples. The mean zeta potential value of free MSN is -25.0 mV. This result of MSN is due to the high amount of silanol groups on the silica surface (Freitas, 2017). However, for MSNAPTES particles, the value was +29.9 mV. Changes could be attributed to insertion of amino group. The results indicate the successfully modification of APTES on the outer surface of the matrices. After kojic acid incorporation, the values of positive potential charge remained positive. Size and dispersion of the particles was confirmed by photon correlation spectroscopy. With this analysis it was possible to see that the sample, after functionalized and incorporated with kojic acid, showed better dispersion with P.D.I around 0.3 (Table 1).

Table 1: Percentage of weight loss, elemental analysis, photon correlation spectroscopy and zeta potential of MSN, MSNAPTES, MSNAPTES KA samples.

Samples	Weight (% w/w) 25-150 ºC	Weight (% w/w) 150-700 ºC	Carbon (%)	Nitrogen (%)	Size	P.D.I.	ζ potencial (mV)
MSN	3.8	3.1	0.4	0.01	692	0.7	-25.0
MSNAPTES	9.9	13.7	8.9	3.0	196	0.2	+29.9
MSNAPTES KA	10.0	18.0	10.2	2.9	218	0.3	+31.3

3.4 Scanning electron microscopy (SEM)

Figure 3 shows the SEM images of MSN and MSNAPTES samples. SEM images of MSN illustrate the presence of homogeneous spherical shaped nanoparticles, with an average diameter around 200-400nm.

(a) 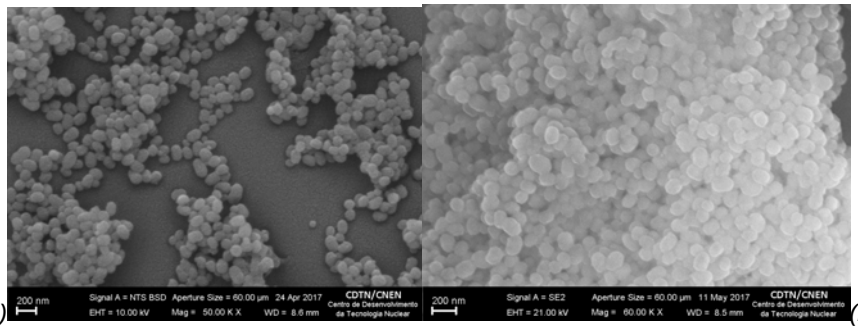 (b)

Figure 3: SEM images of MSN (a) and MSNAPTES (b) samples with spherical structure.

3.5 Biologic assays

In the present study, KA alone and loaded to MSNAPTES were tested in AChE, tyrosinase and antimicrobial inhibitory activity the analysis results are shown in Tables 2 and 3.

Table 2: Inhibitory percent of nanoparticles in AChE and tyrosinase inhibitory activity.

Samples	AChE inhibition (%) ± SD	Tyrosinase inhibition (%) ± SD
MSNAPTES	inactive	inactive
MSN	inactive	inactive
MSNAPTES KA	66.28 ± 1.55	28.57 ± 0.20
KA	80.28 ± 1.31	98.50 ± 1.80
Galantamine	94.34 ± 1.06	Do not apply

Table 3: Inhibitory percent of nanoparticles in antimicrobial assay.

	% of inhibition				
Samples	*C. albicans*	*E. coli*	*S. aureus*	*S. enterica*	*B. cereus*
MSNAPTES KA	18.42 ± 1.80	0	54.45 ± 4.30	20.96± 3.07	13.48 ± 4.3
MSNAPTES	0	0	0	0	0
MSN	0	0	0	0	0
Chloranphenicol	do not apply	99.30 ± 1.45	95.57 ± 0.27	96.11 ± 0.32	93.34 ± 2.00
Itraconazole	96.98 ± 3.13	do not apply	do not apply	do not apply	do not apply

MSNAPTES was screened, and in all assays, it was found that this base did not show any activity. KA revealed as a new promising AChE inhibitor, enzyme associated to Alzheimer's disease. In addition in the nanoparticles activity MSNAPTES KA was able to inhibit 66.28 ± 1.55% of this enzyme, showing that the activity presented by KA was preserved after KA loading. KA is also widely used as an inhibitor of tyrosinase, enzyme involved in melanin biosynthesis. The incorporation of KA in MSNAPTES led to the preservation of its activity. In antimicrobial assay, KA inhibited the growth of *C. albicans* and *S. aureus* above 50% and KA loading was able to inhibited growing of this microorganisms. KA can be easily oxidized and degraded by enzymes present in the body and may not exert its function. The MSNAPTESKA showed size in the nanometric scale, as can be observed by microscopy (SEM) and the concentration of 3% of kojic acid, that was obtained by the TG and CHN analyzes. The size presented by the nanoparticle favors the passage through the body and its passage through the membranes, such as hematoencephalic barriers, as well as the presence of pores promotes acid protection against enzymatic action. The concentration of KA present in the nanoparticle is much lower than the free acid concentration (1.0 mg mL^{-1}) used in the assay, which indicates that in the nanoparticle the KA efficiency increases. These studies show that the incorporation of KA in MSNAPTES preserves the biological activity of this important compound. Therefore, this could be a strategy on nanomaterials to achieve important diseases like Alzheimer's and microbial infections.

4. Conclusions

In this study, we have demonstrated the effective loading process of kojic acid, an important bioactive fungal metabolite, in mesoporous silica functionalized with APTES. The nano-system synthesized (MSNAPTESKA) showed to contain an estimated concentration of 3% of kojic acid. Although MSNAPTES KA present thirty

times less amount of kojic acid than the free-acid, when biological activity of this nanoparticle was evaluated against susceptible bacteria, it maintained high antibacterial action against *C. albicans, S. aureus*, *S. enterica* and *B. cereus.* These results are promising since the nano-system activity profile was similar to the results obtained for free-kojic acid. In relation to AChE inhibition test, efficient inhibition by MSNAPTESKA nanoparticles was also verified. Furthermore, it was observed that KA loading has preserved tyrosine's inhibitory property. Therefore, the results indicate that this nanoparticle, which has advanced stability over free-kojic acid degradation, maintains the biological activity profile of free-KA, being, therefore, a very promising lead for cosmetic, food and pharmaceutical industry development.

Acknowledgments

The authors thank Fundação de Amparo à Pesquisa do estado de Minas Gerais (FAPEMIG), Conselho Nacional de Desenvolvimento Científico e Tecnológico (CNPq) and Coordenação de Aperfeiçoamento de Pessoal de Nível Superior (CAPES) for financial help.

Reference

Ashraf Z., Rafiq M., Seo S.-Y., Babar M.M., Zaidi N.-us-S.S., 2015, Design, synthesis and bioevaluation of novel umbelliferone analogues as potential mushroom tyrosinase inhibitors, J Enzyme Inhib. Med. Chem. 30 (6), 874-883.

Bentley R., 2006, From miso, sake and shoyu to cosmetics: a century of science for kojic acid, Nat. Prod. Rep. 23, 1046-1062.

Burnett C.L., Bergfeld W.F., Belsito D.V., Hill R.A., Klaassen C.D., Liebler D.C., Marks J.G., Shank R.C., Slaga T.J., Snyder P.W., Andersen A., 2010, Final report of the safety assessment of kojic acid as used in cosmetics, Int. J. Toxicol. 29 (4), 244S -273S.

Dos Santos G.F., Pereira R.G., Boaventura M.A.D., Macias F.A., Lima G.S., Coelho A.C.S., Molinillo J.M.G., Cala A., Takahashi J.A., 2017, Structure-activity relationship study of diterpenes for treatment of Alzheimer's disease, Quim. Nova, 1-6. *In press*.

Fan J., Fang G., Wang X., Zeng F., Xiang Y., Wu S., 2011, Targeted anticancer prodrug with mesoporous silica nanoparticles as vehicles, Nanotechnology, 22 (45), 1-11.

Food and Drug Administration (FDA). Briefing document, *FDA database*. 2016.

Freitas L.B.O., Corgosinho L.M., Faria J.A.Q.A., dos Santos V.M., Resende J.M., Leal A.S., Gomes D.A., de Souza E.M.B., 2017, Multifunctional mesoporous silica nanoparticles for cancer-targeted, controlled drug delivery and imaging, Microporous Mesoporous Mater. 242, 271-283.

Izquierdo-Barba I., Sousa E., Doadrio J.C., Doadrio A.L., Pariente J.P., Martínez A., Babonneau F., Vallet-Regi M., 2009, Influence of mesoporous structure type on the controlled delivery of drugs: release of ibuprofen from MCM-48, SBA-15 and functionalized SBA-15. J. Solgel Sci. Technol. 50 (3), 421–429.

Kim J.M., Chang S.M., Kong S.M., Kim K.-S., Kim J., Kim W.-S., 2009, Control of hydroxyl group content in silica particle synthesized by the sol-precipitation process, Ceram. Int. 35 (3), 1015-1019.

Mohamad R., Mohamed M.S., Suhaili N., Salleh M.M., Ariff A.B., 2010, Kojic acid: Applications and development of fermentation process for production, Biotechnol. Mol. Biol. Rev. 5 (2), 24-37.

Nohynek G.J., Kirkland D., Marzinc D., Toutain H., Leclerc-Ribaud C., Jinnai H., 2004, An assessment of the genotoxicity and human health risk of topical use of kojic acid [5-hydroxy-2-(h ydroxymethyl)-4H-pyran-4-one], Food Chem. Toxicol. 42, 93-105.

Vallet-Regi M., Rámila A., del Real R.P., Perez-Pariente J., 2001, A new property of MCM-41: Drug delivery system, Chem. Mater. 13 (2), 308-311.